ed to clearly establish the dependence of the field strength on the value of x.

We define a temperature T^*_{ZF} at which the onset of spontaneous magnetic fields is observed, and this is plotted versus the oxygen content x along with $T_c(x)$ in Fig. 4. At $x = 0.67$, T^*_{ZF} is between the pseudogap transition $T^* \approx 140$ K determined from the peak in the ^{63}Cu NMR spin-lattice relaxation rate $1/T_1T$ (*30*) and the departure of the resistivity $\rho(T)$ from linearity (*31*), and $T^* \approx 200$ K estimated from the downturn in the ^{89}Y NMR Knight shift (*32*). The hole concentration p can be estimated from the following empirical equation (*33*)

$$T_c = T_{c,max}[1 - 82.6(p - 0.16)^2] \quad (2)$$

The inset of Fig. 4 is a plot of T_c and T^*_{ZF} versus the hole concentration p. If one assumes a linear extrapolation through the data points of $T^*_{ZF}(p)$ corresponding to $x = 0.67$ and $x = 0.95$, T^*_{ZF} falls to zero at a critical doped-hole concentration of $p_{cr} = 0.182 \pm 0.009$.

Our investigation of highly pure and homogeneous crystals of $YBa_2Cu_3O_{6+x}$ reveals the onset of spontaneous static magnetic fields at a temperature dependent on the oxygen content x. In the underdoped sample, the onset is near the pseudogap crossover temperature T^* deduced from other methods, whereas the onset occurs well below T_c at optimal doping. Although the occurrence of magnetic moments below T^* is consistent with some recent theories of the pseudogap phase, the increased ZF relaxation rate is too small to clearly determine whether the static fields arise from a dilute or dense concentration of magnetic moments.

References and Notes

1. R. E. Walstedt, W. W. Warren Jr., *Science* **248**, 1082 (1990).
2. J. M. Tranquada, P. M. Gehring, G. Shirane, S. Shamoto, M. Sato, *Phys. Rev. B* **46**, 5561 (1992).
3. N. Nishida *et al.*, *Jpn. J. Appl. Phys.* Pt. 2 **26**, L1856 (1987).
4. N. Nishida *et al.*, *J. Phys. Soc. Jpn.* **57**, 599 (1988).
5. J. H. Brewer *et al.*, *Phys. Rev. Lett.* **60**, 1073 (1988).
6. R. F. Kiefl *et al.*, *Phys. Rev. Lett.* **63**, 2136 (1989).
7. P. Dai *et al.*, *Science* **284**, 1344 (1999).
8. W. W. Warren, *Phys. Rev. Lett.* **62**, 1196 (1989).
9. J. W. Loram, K. A. Mirza, J. R. Cooper, W. Y. Liang, J. M. Wade, *J. Supercond.* **7**, 243 (1994).
10. V. J. Emery, S. A. Kivelson, *Nature* **374**, 434 (1995).
11. J. L. Tallon, J. W. Loram, *Physica C* **349**, 53 (2001).
12. C. Varma, *Phys. Rev. B* **55**, 14554 (1997).
13. ———, *Phys. Rev. Lett.* **83**, 3538 (1999).
14. S. Chakravarty, R. B. Laughlin, D. K. Morr, C. Nayak, *Phys. Rev. B* **64**, 094503 (2001).
15. T. C. Hsu, J. B. Marston, I. Affleck, *Phys. Rev. B* **43**, 2866 (1991).
16. X.-G. Wen, P. A. Lee, *Phys. Rev. Lett.* **76**, 503 (1996).
17. J. B. Marston, A. Sudbø, preprint available at http://xxx.lanl.gov/abs/cond-mat/0103120.
18. A. Amato, *Rev. Mod. Phys.* **69**, 1119 (1997).
19. R. F. Kiefl *et al.*, *Phys. Rev. Lett.* **64**, 2082 (1990).
20. Y. Sidis *et al.*, *Phys. Rev. Lett.* **86**, 4100 (2000).
21. H. A. Mook, P. Dai, F. Dogan, preprint available at http://xxx.lanl.gov/abs/cond-mat/0102047.
22. The HELIOS spectrometer uses a large superconducting solenoid, so that true ZF measurements could only be obtained at temperatures below T_c where small stray external fields are excluded from the bulk by the Meissner screening currents flowing around the perimeter of the sample. The LAMPF spectrometer consists of three orthogonal pairs of Helmholtz coils, which allow us to zero the field in the normal state to better than 0.1 G in each of the $\hat{x}$, $\hat{y}$, and $\hat{z}$, directions. In the latter setup, a mosaic of single crystals was mounted on a high-purity Ag backing and sandwiched between a thin muon detector and a light guide, all of which was contained within a ^{4}He gas-flow cryostat. This arrangement ensured that all sources of signal relaxation originated from within the sample.
23. R. Liang *et al.*, *Physica C* **195**, 51 (1992).
24. R. Liang, D. A. Bonn, W. N. Hardy, *Physica C* **336**, 57 (2000).
25. R. Kubo, T. Toyabe, in *Magnetic Resonance and Relaxation*, R. Blinc, Ed. (North-Holland, Amsterdam, 1967).
26. J. H. Brewer *et al.*, *Hyperfine Interactions* **63**, 177 (1990).
27. N. Nishida, H. Miyatake, *Hyperfine Interactions* **63**, 183 (1990).
28. N. Weber *et al.*, *Hyperfine Interactions* **63**, 207 (1990).
29. C. Boekema, W. K. Dawson, D. W. Cooke, *Hyperfine Interactions* **86**, 519 (1994).
30. M. Takigawa *et al.*, *Phys. Rev. B* **43**, 247 (1991).
31. B. Wuyts, V. V. Moshchalkov, Y. Bruynseraede, *Phys. Rev. B* **53**, 9418 (1996).
32. H. Alloul, T. Ohno, P. Mendels, *Phys. Rev. Lett.* **63**, 1700 (1989).
33. J. L. Tallon, C. Bernhard, H. Shaked, R. L. Hitterman, J. D. Jorgensen, *Phys. Rev. B* **51**, 12911 (1995).

34. H. Claus, S. Yang, A. P. Paulikas, J. W. Downey, B. W. Veal, *Physica C* **171**, 205 (1990).
35. We gratefully acknowledge S. Chakravarty, J. B. Marston, D. Morr, P. Stamp, I. Affleck, and G. M. Luke for helpful and informative discussions. J.H.B., R.F.K., D.A.B., W.N.H., and R.L. acknowledge support from the Canadian Institute for Advanced Research. C.E.S. acknowledges support from the U.S. Air Force Office of Scientific Research grant F49620-97-1-0297.

19 March 2001; accepted 26 April 2001

Geometric Manipulation of Trapped Ions for Quantum Computation

L.-M. Duan,* J. I. Cirac, P. Zoller

We propose an experimentally feasible scheme to achieve quantum computation based solely on geometric manipulations of a quantum system. The desired geometric operations are obtained by driving the quantum system to undergo appropriate adiabatic cyclic evolutions. Our implementation of the all-geometric quantum computation is based on laser manipulation of a set of trapped ions. An all-geometric approach, apart from its fundamental interest, offers a possible method for robust quantum computation.

The physical implementation of quantum computers requires a series of accurately controllable quantum operations on a set of two-level systems (qubits). These controllable quantum operations can be either of the traditional dynamical origin (*1*) or of a novel geometric origin (*2–7*). The all-geometric approach, proposed recently with the name of holonomic quantum computation (*4–7*), achieves the whole set of universal quantum gates solely based on the Abelian and non-Abelian geometric operations (holonomies), without any contributions from dynamical gates. The holonomies are acquired when a quantum system is driven to undergo some appropriate cyclic evolutions by adiabatically changing the controllable parameters in the governing Hamiltonian (*8–10*). The holonomies can be either simple Abelian (commutable) phase factors (Berry phases) or general non-Abelian operations, depending on whether the eigenspace of the governing Hamiltonian is nondegenerate or degenerate. Besides its fundamental interest related to a general geometric global structure, the holonomic quantum computation scheme has some built-in fault-tolerant features (*2*, *7*), which might offer practical advantages, such as being resilient to certain types of computational errors. Several schemes have been proposed for the geometric realization of the particular conditional phase shift gate with the use of the Abelian Berry phase (*2*, *3*), and one of them has been experimentally demonstrated with the nuclear magnetic resonance technique (*2*). For a universal quantum computation, one still needs to combine this particular geometric gate with some single-bit dynamical gates (*11*). We propose an experimentally feasible scheme to achieve the universal quantum computation all by the geometric means. This requires us to realize the non-Abelian holonomies as well as the Abelian ones, because the universal set of quantum gates is necessarily noncommutable. Our scheme, which is based on laser manipulation of a set of trapped ions, fulfills all the requirements for holonomic quantum computation and fits well the status of current technology.

For the holonomic quantum computation proposed recently (*4–7*), the computational space C is always an eigenspace (highly degenerate) of the governing Hamiltonian, with a

Institute for Theoretical Physics, University of Innsbruck, A-6020 Innsbruck, Austria.

*To whom correspondence should be addressed. E-mail: Luming.Duan@uibk.ac.at

trivial eigenvalue 0. Though the Hamiltonian restricted to the computational space is completely trivial and there is no dynamical evolution at all, the dependence of the Hamiltonian on some controllable adiabatically changing parameters makes the space C undergo a highly nontrivial evolution due to the global geometric structure in the parameter space. In fact, one requires any unitary operations in the space C to be obtainable by these geometric evolutions in order to achieve universal quantum computing. It is well known that some single-qubit operations, together with a nontrivial two-bit gate, make a universal set of gate operations for quantum computing (*11*). It is enough for us to construct some looped paths in the parameter space to achieve the desired geometric evolutions corresponding to these gate operations, and then a composition of these parameter loops suffices to obtain an arbitrary unitary evolution in the computational space C. Here we show how to achieve all the desired geometric gate operations using a set of trapped ions. The schemes for ion-trap quantum computers based on the conventional dynamical evolutions have been proposed (*12*–*15*), and some single-bit and multi-bit gate operations have been demonstrated experimentally (*16*–*18*). We use the same setup, but we use it to achieve holonomic quantum computation. We also note that an idealized scheme (*19*) was recently proposed for holonomic quantum computation. To the best of our knowledge, our proposal is the first realistic one that achieves all the elements of holonomic quantum computation and is feasible with current technology.

We choose the universal set of gate operations to be $U_1^{(j)} = e^{i\phi_1|1\rangle_j\langle 1|}$, $U_2^{(j)} = e^{i\phi_2\sigma_j^y}$, and $U_3^{(jk)} = e^{i\phi_3|11\rangle_{jk}\langle 11|}$, where $|0\rangle_j$ and $|1\rangle_j$ constitute the computational basis for each qubit, $\sigma_j^y = i(|1\rangle_j\langle 0| - |0\rangle_j\langle 1|)$ is the Pauli operator of the j qubit, and ϕ_1, ϕ_2, ϕ_3 are arbitrary phases. The universality of this set of gates follows directly from the proof in (*11*) and is well known. First we show how to realize the single-bit gates $U_1^{(j)}$ and $U_2^{(j)}$ geometrically. The system we have in mind is a set of ions confined in a linear Pauli trap (*12*, *17*, *18*). Each ion has three ground (or metastable) states $|0\rangle$, $|1\rangle$, and $|a\rangle$, and one excited state $|e\rangle$ (Fig. 1). The state $|a\rangle$ is used as an ancillary level for gate operations. The ground states could be different hyperfine levels or in the same manifold but with different Zeeman sublevels, and they are coupled to the excited state $|e\rangle$ separately by a resonant classical laser with a different polarization or frequency (a possible separate addressing of the three levels is shown in Fig. 1). The Hamiltonian for each ion with the laser on has the form

$$H_j = \hbar\,[\,|e\rangle_j\,(\Omega_0\langle 0| + \Omega_1\langle 1| + \Omega_a\langle a|) + \text{h.c.}] \quad (1)$$

in the rotating frame, where Ω_0, Ω_1, Ω_a are Rabi frequencies serving as the controlling parameters, and h.c. represents the Hermitian conjugate term. The Hamiltonian in the rotating frame is independent of the laser frequencies, because all the lasers are resonant with the corresponding level transitions. The parameters Ω_0, Ω_1 should be set to zero initially so that the computational space spanned by $|0\rangle_j$ and $|1\rangle_j$ is initially an eigenspace of the gate Hamiltonian with a zero eigenvalue. Then the three Rabi frequencies make an adiabatic cyclic evolution in the parameter space M with the change rate significantly smaller than the typical Rabi frequencies (the adiabatic condition), and the adiabatic theorem ensures that the computational space remains the eigenspace of the gate Hamiltonian with the zero eigenvalue, so there is no dynamical phase contribution at all. However, we will explicitly show that the topological holonomies accompanying the adiabatic evolutions suffice for construction of the gates $U_1^{(j)}$ and $U_2^{(j)}$, which in fact shows that any single-bit operation is obtainable by such holonomies.

To get the gate $U_1^{(j)}$, we set $\Omega_0 = 0$ so that the state $|0\rangle_j$ is decoupled, and choose $\Omega_1 = -\Omega\sin\frac{\theta}{2}e^{i\varphi}$, $\Omega_a = \Omega\cos\frac{\theta}{2}$. The relative amplitude θ and phase φ of the Rabi frequencies Ω_1 and Ω_a are the effective control parameters, and the absolute magnitude Ω is irrelevant for the gate control as long as it is large enough to satisfy the adiabatic condition, which could be a good feature for real experiments. The dark state (the eigenstate with the zero-energy eigenvalue) of the gate Hamiltonian has the form $\cos\frac{\theta}{2}|1\rangle_j + \sin\frac{\theta}{2}e^{i\varphi}|a\rangle_j$, where the parameters θ,φ make a cyclic evolution with the starting and ending point to be $\theta = 0$. Using the standard formula for the geometric phase (*8*, *10*), we can show that this cyclic evolution achieves the gate operation $U_1^{(j)}$ with the acquired Berry phase $\phi_1 = \oint \sin\theta d\theta d\varphi$. This evolution has a definite geometric interpretation: The acquired Berry phase is exactly the enclosed solid angle $\oint d\Omega$ swept by the vector always pointing to the (θ,φ) direction. From this interpretation, one immediately sees that the gate operation is determined only by the global property (that is, the swept solid angle) and does not depend on the details of the evolution path in the parameter space. This is an advantage of holonomic quantum computation, which makes it robust against certain types of errors. For instance, the local random errors along the evolution path caused by some unwanted interaction would have very small influence on the global property.

Now we show how to achieve the gate $U_2^{(j)}$ geometrically. For this purpose, we choose $\Omega_0 = \Omega\sin\theta\cos\varphi$, $\Omega_1 = \Omega\sin\theta\sin\varphi$, and $\Omega_a = \Omega\cos\theta$ in the Hamiltonian (Eq. 1), with the parameters θ,φ similarly undergoing an adiabatic cyclic evolution from $\theta = 0$ to $\theta = 0$. The two degenerate dark states of this gate Hamiltonian have the form $|D_1\rangle = \cos\theta(\cos\varphi|0\rangle_j + \sin\varphi|1\rangle_j) - \sin\theta|a\rangle_j$ and $|D_2\rangle = \cos\varphi|1\rangle_j - \sin\varphi|0\rangle_j$, from which we can show, by using the formula for holonomies (*6*, *9*), that the cyclic evolution of θ,φ achieves the gate operation $U_2^{(j)}$ with the phase $\phi_2 = \oint d\Omega$, the swept solid angle by the vector (θ,φ). The ability to obtain both of the noncommutable geometric gates $U_1^{(j)}$ and $U_2^{(j)}$ in fact shows that one constructs non-Abelian holonomies, because the composite holonomies of the $U_1^{(j)}$ and $U_2^{(j)}$ and of the $U_2^{(j)}$ and $U_1^{(j)}$ are different. Although the Abelian holonomies have been tested experimentally by various means (*10*, *20*), the controllable demonstration of the non-Abelian ones is believed to be more complicated (*10*, *19*). Here, in contrast, we introduce a simple way to test this fundamental effect by manipulating a single ion with a laser. In fact, for the demonstration of the non-Abelian holonomies, we do not need to exploit any interaction between the ions, so one can also use a sample of free particles instead of a single ion for a simple test. For instance, one can experimentally verify this by laser manipulation of a cloud of atoms in a magnetic-

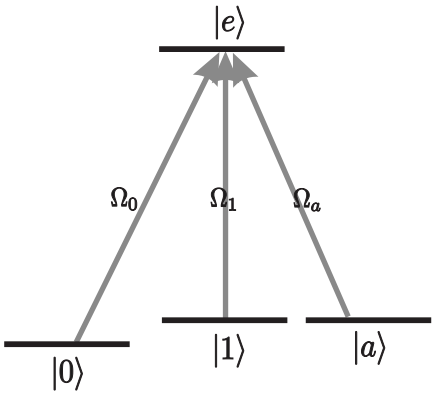

Fig. 1. Level structure and laser configuration for single-bit operations. A possible choice for the three ground or metastable states is that $|1\rangle$ and $|a\rangle$ are two degenerate Zeeman sublevels that are addressed by lasers with different polarizations, and $|0\rangle$ is the ground state (another hyperfine level) with slightly different energy, so that it can be addressed by a laser with a different frequency.

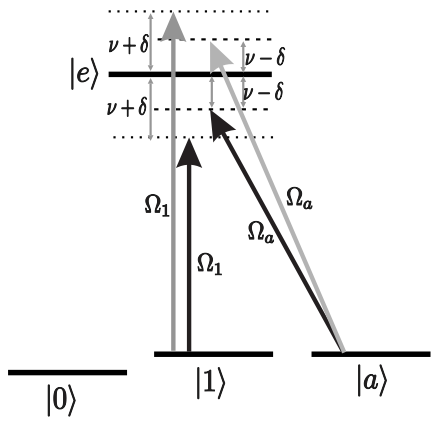

Fig. 2. Laser configuration for the two-bit operation. The same configuration is used for both ions.

optical trap, which is readily available in many laboratories.

A combination of the gates $U_1^{(j)}$ and $U_2^{(j)}$ permits us to implement any single-bit operation, which together with the nontrivial two-bit gate $U_3^{(jk)}$ between the qubits j,k are enough for universal quantum computation. To construct the gate $U_3^{(jk)}$ using geometric means, we need to exploit the Coulomb interactions between the ions. For this purpose, we provide a scheme based on a recent dynamical proposal (*14*), which uses two-color laser manipulation. The transition $|1\rangle \rightarrow |e\rangle$ for the j,k ions is driven by a red and a blue detuned laser, respectively, with detunings $-(\nu + \delta)$ and $\nu + \delta$ (Fig. 2), where ν is the phonon frequency of one oscillation mode (normally the center of mass mode) and δ is an additional detuning. Similarly, the transition $|a\rangle \rightarrow |e\rangle$ is also driven by a red and a blue detuned laser, but with the additional detuning $\delta' \neq \delta$ to avoid the direct Raman transition. For simplicity, here we choose $\delta' = -\delta$ as in Fig. 2. Under the condition of strong confinement $\eta^2 \ll 1$ (the Lamb-Dicke criterion), where η is defined by the ratio of the ion oscillation amplitude to the manipulation optical wave length, the Hamiltonian describing the interaction has the form

$$H_{jk} = \frac{\eta^2}{\delta}\left[-|\Omega_1|^2\sigma_{j1}^{\varphi_1}\sigma_{k1}^{\varphi_1} + |\Omega_a|^2\sigma_{ja}^{\varphi_a}\sigma_{ka}^{\varphi_a}\right], \quad (2)$$

where $\sigma_{j\mu}^{\varphi_\mu} \equiv e^{i\varphi_\mu}|e\rangle_j\langle\mu| + \text{h.c.}$ ($\mu = 1,a$) and Ω_1, Ω_a are the corresponding Rabi frequencies, respectively, with the phases φ_1, φ_a. In writing the Hamiltonian (Eq. 2), we have neglected some trivial light shift terms that can be easily compensated, for instance, by another laser. To get a geometric operation, we choose the relative intensity $|\Omega_1|^2/|\Omega_a|^2 = \tan(\theta/2)$ and phase $\varphi_1 - \varphi_a = \varphi/2$, with the control parameters θ,φ undergoing a cyclic adiabatic evolution from $\theta = 0$. During the evolution, the computational bases $|00\rangle_{jk}$, $|01\rangle_{jk}$, and $|10\rangle_{jk}$ are decoupled from the Hamiltonian (Eq. 2), while the $|11\rangle_{jk}$ component adiabatically follows as $\cos\frac{\theta}{2}|11\rangle_{jk} + \sin\frac{\theta}{2}e^{i\varphi}|aa\rangle_{jk}$, which acquires a Berry phase after the whole loop. So we get the conditional phase-shift gate $U_3^{(jk)}$ with the purely geometric phase $\phi_3 = \oint d\Omega$, the swept solid angle by the vector (θ,φ). This geometric two-bit gate has shared the advantages of the recently proposed and demonstrated dynamical scheme (*14*, *18*) in the sense that, first, the ion motional modes need not be cooled to their ground states as long as the Lamb-Dicke criterion is satisfied; and second, separate addressing of the ions is not needed during the two-bit gate operation.

For experimental demonstration of the above universal set of geometric gates, we need to consider several kinds of decoherence that impose concrete conditions on the relevant parameters. First, one should fulfill the adiabatic condition. This means the gate operation time should be larger than the inverse of the energy gap between the dark states and the bright and excited states. The energy gap is given by $\Delta_1 = |\Omega|$ for the single-bit gates and by $\Delta_2 = \eta^2|\Omega|^2/\delta$ for the two-bit gate. So we require that the single-bit and two-bit gate operation times t_i^g ($i = 1, 2$) be reasonably long, so that the leakage error to the bright and the excited states, which scales as $1/(\Delta_i t_i^g)^2$, is small. Second, we need to avoid spontaneous emission (with a rate γ_s) of the excited state $|e\rangle$. Because of the adiabatic condition, the excited state is only weakly populated even though we use resonant laser coupling, and the effective spontaneous emission rate is reduced by the leakage probability $1/(\Delta_i t_i^g)^2$. As a result, we only require $\gamma_s/(\Delta_i^2 t_i^g) \ll 1$ for the spontaneous emission to be negligible during the gate operation. Finally, the influence of the heating of the ion motion should be small. We assume that all the manipulation lasers are copropagating, so that the heating caused by the two-photon recoils is negligible. The carrier phononic states are only virtually excited during the two-bit gate, so the influence of the heating rate γ_h is reduced by the phonon population probability $\eta^2|\Omega|^2/\delta^2$. The effective heating rate should be much smaller than the gate speed, which requires $\delta \gg \gamma_h$. All the conditions discussed above in the geometric gates are exactly parallel to those in the dynamical schemes using the off resonant Raman transitions. The reason for this is that, in both cases, the excited state is only weakly populated and the population probability obeys the same scaling law, although the physical mechanism for the weak population is quite different. So, compared with the dynamical schemes, our requirements are not more stringent. However, the geometric proposal introduced in this paper will permit us to experimentally investigate the fundamental Abelian and non-Abelian holonomies (*10*) and may open new possibilities for robust quantum computation (*21*, *22*).

References and Notes

1. D. P. DiVincenzo, *Science* **270**, 255 (1995).
2. J. A. Jones, V. Vedral, A. Ekert, G. Castagnoli, *Nature* **403**, 869 (1999).
3. G. Falci *et al.*, *Nature* **407**, 355 (2000).
4. P. Zanardi, M. Rasetti, *Phys. Lett. A* **264**, 94 (1999).
5. J. Pachos, P. Zanardi, M. Rasetti, *Phys. Rev. A* **61**, 010305(R) (2000).
6. J. Pachos, Lawrence Berkeley National Laboratory (LANL) preprint available at http://xxx.lanl.gov/abs/quant-ph/0003150.
7. J. Pachos, P. Zanardi, LANL preprint available at http://xxx.lanl.gov/abs/quant-ph/0007110.
8. M. V. Berry, *Proc. R. Soc. London A* **392**, 45 (1984).
9. F. Wilczek, A. Zee, *Phys. Rev. Lett.* **52**, 2111 (1984).
10. A. Shapere, F. Wilczek, *Geometric Phases in Physics* (World Scientific, Singapore, 1989).
11. S. Lloyd, *Phys. Rev. Lett.* **75**, 346 (1995).
12. J. I. Cirac, P. Zoller, *Phys. Rev. Lett.* **74**, 4091 (1995).
13. A. Sorensen, K. Molmer, *Phys. Rev. Lett.* **82**, 1971 (1999).
14. K. Molmer, A. Sorensen, *Phys. Rev. Lett.* **82**, 1835 (1999).
15. J. I. Cirac, P. Zoller, *Nature* **404**, 579 (2000).
16. C. Monroe *et al.*, *Phys. Rev. Lett.* **75**, 4714 (1995).
17. Ch. Roos *et al.*, *Phys. Rev. Lett.* **83**, 4713 (1999).
18. C. A. Sackett *et al.*, *Nature* **256**, 256 (2000).
19. J. Pachos, S. Chountasis, *Phys. Rev. A* **62**, 052318-1 (2000).
20. P. G. Kwiat, R. Y. Chiao, *Phys. Rev. Lett.* **66**, 588 (1991).
21. A. Y. Kitaev, LANL preprint available at http://xxx.lanl.gov/abs/quant-ph/9707021.
22. J. Preskill, LANL preprint available at http://xxx.lanl.gov/abs/quant-ph/9712048.

23. We thank P. Zanardi and J. Pachos for helpful discussions. Supported by the Austrian Science Foundation, the Europe Union project EQUIP, the European Science Foundation, the European TMR network Quantum Information, and the Institute for Quantum Information.

8 January 2001; accepted 11 April 2001

Explaining the Weddell Polynya—a Large Ocean Eddy Shed at Maud Rise

D. M. Holland

Satellite observations have shown the occasional occurrence of a large opening in the sea-ice cover of the Weddell Sea, Antarctica, a phenomenon known as the Weddell Polynya. The transient appearance, position, size, and shape of the polynya is explained here by a mechanism by which modest variations in the large-scale oceanic flow past the Maud Rise seamount cause a horizontal cyclonic eddy to be shed from its northeast flank. The shed eddy transmits a divergent Ekman stress into the sea ice, leading to a crescent-shaped opening in the pack. Atmospheric thermodynamical interaction further enhances the opening by inducing oceanic convection. A sea-ice–ocean computer model simulation vividly demonstrates how this mechanism fully accounts for the characteristics that mark Weddell Polynya events.

The Weddell Polynya—the largest observed sea-ice anomaly of the polar oceans—is a hole in the sea-ice cover of the Weddell Sea, Antarctica, that can occupy an area of well over 200,000 km^2, a size comparable to the island of Great Britain. The appearance of

Geometric Manipulation of Trapped Ions for Quantum Computation

L.-M. Duan, J. I. Cirac and P. Zoller

Science **292** (5522), 1695-1697.
DOI: 10.1126/science.1058835